EXPERIMENTAL INVESTIGATION ON THE EFFECT OF WATER DEPTH ON ROLL NATURAL PERIOD AND DAMPING COEFFICIENT OF LARGE COMMERICAL SHIPS IN SHALLOW WATER REGIONS

Javad A. Mehr, Australian Maritime College, University of Tasmania, Australia
Mohammadreza Javanmardi, OMC International, Australia
Shin Wei Tham and **Yun Yin,** Australian Maritime College, University of Tasmania, Australia

SUMMARY

Extreme drought condition has led to a low water level in rivers and consequently interrupted transportation not only for large vessels but also for the small vessels which could safely passed through the rivers in the past. To avoid grounding and provide safe transits, all possible vertical motions, specifically roll motion due to wind gust and/or rudder deflection during operation inland waterways, should be carefully considered. Natural period and damping coefficient of roll are two essential hydrodynamic parameters for the prediction of roll motion.

The aim of this study is to investigate the effect of water depth on roll natural period and damping coefficient of large commercial ships passing through different water depths. The results show that the roll natural period and damping coefficient are not significantly influenced by the change in water depth for the depth to draft ratio of greater than 2.0. However, the roll period and damping coefficient increase exponentially with the decrease of water depth for the depth to draft ratio of less than 2.0.

NOMENCLATURE

a_{44}	Added moment of inertia (kg·m²)
b_1	Linear damping coefficient (N·m·s)
b_2 and b_3	Nonlinear damping coefficients (N·m·s² and N·m·s³)
b_{eq}	Equivalent linear damping coefficient (N·m·s)
B	Beam (m)
$B(\dot{\varphi}, \varphi)$	Nonlinear damping moment (N·m)
c_1, c_3, c_5	Stiffness coefficients
$C(\varphi)$	Nonlinear restoring moment (N·m)
C_B	Block coefficient
d/t	Water depth to draft ratio
g	Gravitational acceleration (m·s^{-2})
GM_T	Transverse metacentric height from centre of gravity (m)
$\overline{GZ}$	Righting arm (m)
h_f	Distance moved on pendulum weight (m)
I	Roll moment of inertia (kg·m²)
k_{xxhull}	Roll gyradius (m)
KG	Distance of centre of gravity from keel (m)
KM_T	Transverse metacentric height from keel (m)
L_{BP}	Length between perpendiculars (m)
m	Mass (kg)
m_f	Roll frame pendulum weight (kg)
$M(t)$	Roll exciting moment (N·m)
T_1	Oscillation period of empty dynamic frame (s)
T_2	Oscillation period of dynamic frame with model (s)
δ	Damping ratio
Δ	Displacement (kg)
$\Delta_{maxsurf}$	Displacement obtained from Maxsurf (kg)
ω_n	Natural frequency of roll (rad·s^{-1})
φ	Roll angle (rad)
$\dot{\varphi}$	Roll rate (rad·s^{-1})

1 INTRODUCTION

Climate change causes Earth's atmosphere continues to warm, and droughts are becoming more frequent, severe, and pervasive. According to NASA, the American west have had some of the driest conditions on record in the past 20 years (NASA, 2021). The Climate Change and Drought Factsheet (Steffen et al., 2018) shows that drought conditions have been officially declared in over 16% of New South Wales and nearly 58% of Queensland. According to the report, late autumn and early winter rainfall has decreased by 15% in southeast Australia since the 1970s, and southwest Australia would be experiencing the most total reductions in autumn and winter precipitation potentially as high as 50% by the late 21st century.

Drought conditions can negatively affect agriculture, water supplies, energy production, human health, and many other aspects of society. In addition, navigation has become perilous as a result of drought. The water levels of the Paraná River, the second-longest river in South America, are at their lowest since 1944 (BBC News, 2021) which is hampering the transport of goods, and this situation could last for years.

Rhine river faced about 150 centimetres water level drop in July 2019 at critical chokepoint near Frankfurt which caused a restriction in heavy barges transits. The Rhine is the Europe's most important waterway with 800 miles through industrial zones in Switzerland, Germany and the Netherlands, and it is critical to trade in this region (William et al., 2019).

Extreme drought condition has interrupted transportation not only for large vessels but also for the small vessels which could safely passed through the rivers in the past. To provide safe transits, all possible vertical motions and draft changes should be considered. One of the sources of the draft change is the roll motion due to rudder deflection and wind gust. Operating in the rivers requires the vessel to remain in the provided safe course and vessels' rudders are continuously in deflection for course keeping purposes. To accurately predict the vessel's roll motion, the precise estimation of roll natural period and damping are essential. Natural period of the roll is a function of ship stability parameters and added mass moment of inertia in roll motion, while the added mass moment of inertia itself, regardless of the vessel particulars, is dependent on the water depth. Therefore, it is expected that natural period of roll changes with altering water depth. Although there have been extensive studies on the roll motion, there are limited knowledge of the effect of very shallow water depth on the natural roll period due to changing added mass moment of inertia component. In this study, the effect of water depth on roll natural period and damping of large commercial ships in shallow water regions has been investigated.

2 ROLL EQUATION OF MOTION

The rolling motion of a ship can be mathematically modelled by the following second-order, nonlinear differential equation of motion (Mahfouz, 2004):

$$(I + a_{44})\ddot{\varphi} + B(\dot{\varphi}, \varphi) + C(\varphi) = M(t) \quad (1)$$

where φ is the roll angle of the vessel, I is the roll moment of inertia, a_{44} is added moment of inertia, $B(\dot{\varphi}, \varphi)$ is the nonlinear damping moment which is a function of roll angle and roll rate, $C(\varphi)$ is the nonlinear restoring moment which is a function of roll angle, and $M(t)$ is the roll exciting moment. A dot over the variable φ indicates differentiation with respect to time.

The damping can be expressed as the sum of two terms: linear (b_1) and nonlinear (b_2 and b_3) as shown in Equation 2, while in the linear solvers, linear and nonlinear damping coefficients per unit mass moment of inertia are replaced by equivalent linear damping (b_{eq}):

$$\frac{B(\dot{\varphi},\varphi)}{I+a_{44}} = b_1\dot{\varphi} + b_2|\dot{\varphi}|\dot{\varphi} + b_3\dot{\varphi}^3 = b_{eq}\dot{\varphi} \quad (2)$$

The restoring moment is a function of underwater part of ship hull form. It is usually expressed as an odd series in the roll angle. Thus, $C(\varphi)$ can be expressed as:

$$\frac{C(\varphi)}{I + a_{44}} = \frac{\Delta\overline{GZ}(\varphi)}{I + a_{44}} = c_1\varphi + c_3\varphi^3 + c_5\varphi^5 \quad (3)$$

where c_1, c_3 and c_5 are stiffness coefficients per unit mass moment of inertia. Again, in linear solvers, nonlinear terms would be ignored. By substituting Equations 2 and 3 into Equation 1 and neglecting nonlinear terms, the roll equation of motion is:

$$\ddot{\varphi} + b\dot{\varphi} + c\varphi = m(t) \quad (4)$$

$$b = 2\delta\omega_n \text{ , } c = \omega_n^2 \text{ and } m = \frac{M}{I+a_{44}}$$

where δ is damping ratio and ω_n is natural frequency of roll. Therefore, to predict the roll motion, all coefficients in the Equation 4 should be accurately calculated.

$$\omega_n = \sqrt{\Delta \times GM_T / (I + a_{44})} \quad (5)$$

$$\delta = \frac{b}{2(I + a_{44})\omega_n} \quad (6)$$

According to above-mentioned equations, both natural frequency of roll and damping coefficients are function of added mass moment of inertia. Although roll motion has been extensively investigated in the previous studies (Haddara & Wu, 1995), (Taylan, 1996), (Delefortrie & Vantorre, 2021), (Zwart, 2017), (Zhou, Lo, & Tan, 2004) and (Hansch, 2015), to the authors' best knowledge, little studies have been conducted to investigate the effect of water depth on natural frequency and damping coefficient due to change of added mass moment of inertia in the roll motion.

According to ITTC (ITTC, 2011), with assumption that the energy loss due to damping during a half cycle of roll is the same when nonlinear and linear damping are used, linear equivalent damping coefficient (b_{eq}) can be expressed as:

$$b_{eq} = b_1 + \frac{8}{3\pi}\omega_e\varphi_a b_2 + \frac{3}{4}\omega_e^2\varphi_a^2 b_3 \quad (7)$$

ITTC has presented a procedure to estimate the linear and nonlinear damping coefficients from a roll decay test.

$$\Delta\varphi = a\varphi_m + b{\varphi_m}^2 + c{\varphi_m}^3 \quad (8)$$

$$\Delta\varphi = \varphi_{n-1} - \varphi_n$$

$$\varphi_m = [\varphi_{n-1} + \varphi_n]/2$$

φ_n is the absolute value of the roll angle at the time of the n-th extreme value and φ_m is mean roll angle. The coefficients a, b and c are called decay coefficients. The relation between these coefficients and the damping coefficients can be derived (ITTC, 2011):

$$a = \frac{\pi b_1}{2\omega_n} \qquad (9)$$

$$b\frac{180}{\pi} = \frac{4}{3}b_2$$

$$c\left(\frac{180}{\pi}\right)^2 = \frac{3\pi\omega_n}{8}b_3$$

3 EXPERIMENT SETUP

To investigate the effect of water depth on natural frequency of roll and damping component, a series of model tests were conducted in the Model Test Basin at the Australian Maritime College (AMC), Launceston, Tasmania. Roll decay tests were conducted on two scaled models of merchant vessels, including bulk carrier (Marad F) and container (Hoorn) as shown in Figure 1, with initial heel angle of 5, 10 and 13 degrees at five different water depths. Table 1 and
Table 2 show the model particulars and water depth conditions, respectively.

Figure 1. Left: Hoorn (Container ship model), Right: Marad F (Bulk carrier model)

Table 1. Model particulars

Model	L_{BP} [m]	B [m]	T [m]	C_B
Hoorn	2.47	0.320	0.12	0.69
Marad F	2.00	0.364	0.12	0.85

Table 2. Water depths and corresponding depth to draft ratios

Water Depth [m]	d/t
0.60	5.000
0.30	2.500
0.24	2.000
0.18	1.500
0.14	1.167

Prior to experimental tests, the hull forms were modelled in Rhino and were exported to MAXSURF Stability Module to carry out hydrostatic evaluation and obtain hydrostatic parameters as shown in Table 3.

Table 3. Models' Hydrostatics Data

Model	KM_T [m]	$\Delta_{maxsurf}$ [kg]	LCG from stern @ even Keel [m]
Hoorn	0.152	62.1	1.220
Marad F	0.160	74.1	1.150

MAXSURF hydrostatics data were used to ballast the models and achieve desired vertical centre of gravity (KG) and roll gyradius (k_{xxhull}). The models were ballasted to achieve KG of 0.135m and 0.9m, and in-air roll gyradius (k_{xxhull}) of 33-35 and 35-38 percentage of model beam for the Hoorn and Marad F, respectively. The value of KG was obtained through inclining experiments. By determining the models' GM_T, the models' KG was calculated using Equation 10.

$$KG = KM_T - GM_T \qquad (10)$$

The roll frame was then used to determine the hull radius of gyration (k_{xxhull}) in percentage of models' beam. Equation 11 was used to calculate the hull radius of gyration.

$$k_{xxhull} = \sqrt{\frac{g \cdot m_f \cdot h_f \cdot ({T_2}^2 - {T_1}^2)}{4\pi^2 \Delta}} \qquad (11)$$

Where m_f is mass of roll frame, Δ is model displacement, h_f is distance moved on pendulum weight, T_1 is oscillation period of empty dynamic frame and T_2 is oscillation period of dynamic frame with model. More information about the roll frame setup and measuring k_{xxhull} can be found in (Dawson, 2015). Figure 2 shows Marad F model on the roll frame after ballast.

Figure 2. Marad F model on the roll frame

The roll decay tests were conducted at the AMC's Model Test Basin (MTB). The MTB has a length of 35m and width of 12m, capable of holding 0-900m water depth. An artificial beach was installed at one end of the basin to mitigate large wave reflection from the basin walls. Besides that, wave absorbing floaters were also deployed at the other three sides of the basin to further compensate wave reflection during the model tests at depth to draft ratios (d/T) of 1.16ȯ, 1.5 and 2.0.

QUALYSIS 3-D optical motion tacking system was used to track and record the models' motions. The system uses 16 fixed reference markers for calibration. 8 cameras record the real-time 6DOF motions by tracking 5 visual trackers fitted to the model, and results could be monitored through the computer screen in real-time as shown in Figure 3.

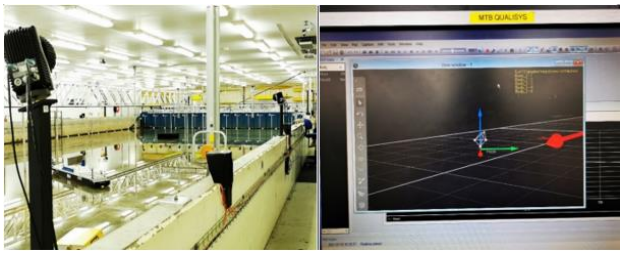

Figure 3. Left: Model test basin and QUALYSIS tracking cameras, Right: QUALYSIS Tracked 3D Vector Field

During the experiment, each model was manually tilted to the designated initial angles of 5, 10 and 13 degrees (monitored through computer screen) then released. The models were allowed to roll freely until the oscillation was visually unobservable through the computer screen. The decay test was conducted at five different water depth to draft ratio of 1.166, 1.5, 2.0, 2.5 and 5 to investigate the effect of water depth on the natural period of roll and damping coefficient. In order to observe the similarity and eliminate uncertainties due to asymmetry, the models were tilted at both sides, port (PRT) and starboard (STBD), during the experiment. The experiment procedure for the roll decay test followed a flowchart as shown in Figure 4. At least three roll decay tests were conducted for each condition to conduct the uncertainty analysis. The uncertainty analysis using the standard deviation showed an average error of 1.5% which is insignificant and has no impact on the key conclusions of this research.

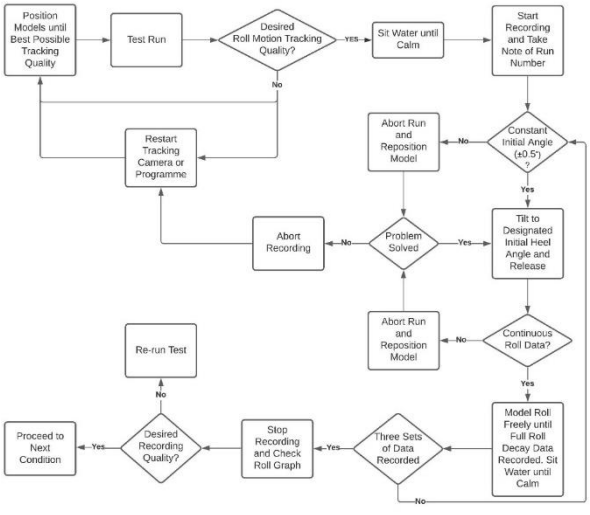

Figure 4. Experiment procedure flowchart

4 RESULTS

4.1 DATA PROCESSING AND ANALYSIS

The raw recorded data from QUALYSIS had to be post-processed to obtain the natural period of the models at different water depths. QUALYSIS cameras captured the 6DOF motion discretely at 200Hz/200 frames per second. Since we were particularly interested in the roll motion, the instantaneous roll angle in degree at each frame was captured, recorded and logged by QUALYSIS. Typical logged roll decay plotted in MATLAB is shown in Figure 5.

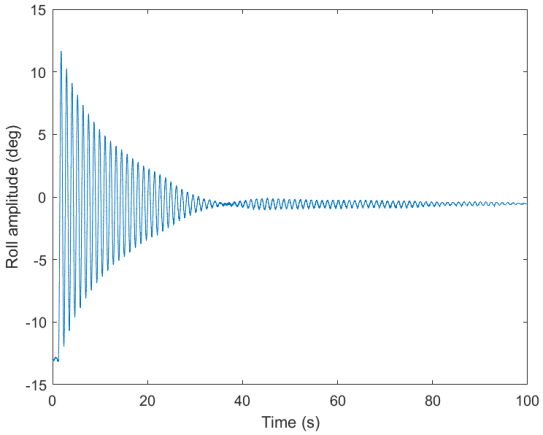

Figure 5. Roll decay test for Marad F at depth to draft ratio of 5, initial heel angle of 13° and portside heel

As explained, the model was tilted manually to the designated initial angle and released. Once released, the model rolled freely and damp naturally from the initial angle to approximately 0 roll degree. However, as shown in the plot (Figure 5), the model resumed rolling shortly after achieving 0 roll degree due to reflected wave in the basin. Therefore, to damp and mitigate the effect of such reflected waves on the model, a waiting period was set before the next roll decay run to ensure the water is perfectly calm.

Fast Fourier Transform (FFT) was applied to transform the time domain data to frequency domain. The frequency with maximum amplitude in the frequency domain curve was taken as the dominated frequency from FFT. The first peak and trough were always excluded from data to eliminate uncertainties due to manual releasing of the tilted model.

The mean value of the dominated periods of each condition for all acceptable decay tests (excluding outliner, >1% difference from mean) was taken as the averaged natural period. In other words, the natural period of a model at certain condition is hence the mean value of the estimated natural period with using FFT from each of three roll decay tests at such condition.

MATLAB fitting toolbox was utilised to fit an exponential curve to the roll decay tests and estimate the damping ratio (δ) as shown in Figure 6. It should be mentioned that roll amplitude less than one degree is excluded, because at a roll motion near its extinction the roll period tends to drift away (Piehl, 2016).

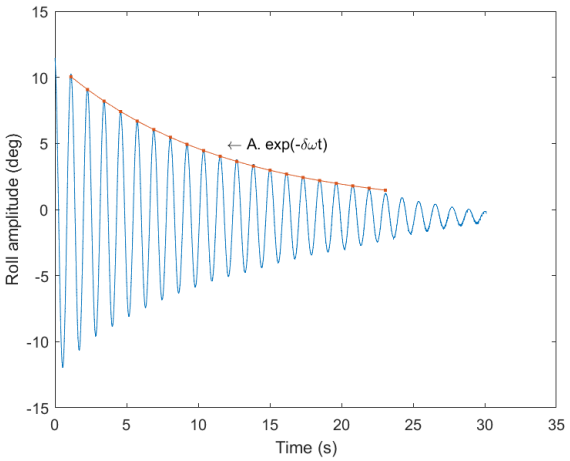

Figure 6. Estimation of damping ratio from roll decay test data

4.2 ROLLING OF HOORN (CONTAINER SHIP MODEL)

The container ship model (Hoorn) was expected to roll at relatively larger period due to higher centre of gravity, shorter metacentric height and smaller roll gyradius in terms of percentage of model's beam. The roll natural periods of the model at different water depths were obtained through roll decay tests and plotted in Figure 7.

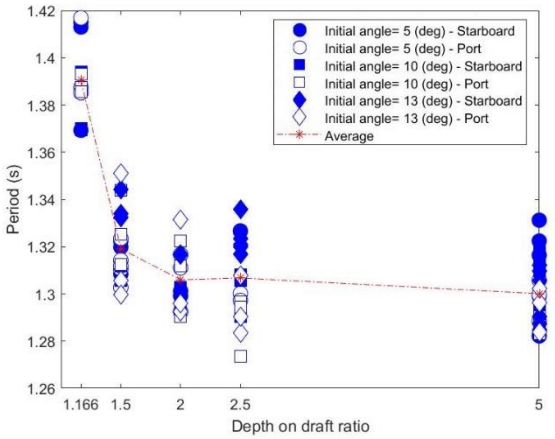

Figure 7. Estimated roll period of container model at different water depth from roll decay tests

As shown, changing in heel side and initial heel angle did not induce significant effect on the roll period of the model at certain water depth.

The estimated damping ratio from roll decay tests for the Hoorn is presented in Figure 8.

According to the results, damping ratio exponentially increases with decreasing the water depth. Similar to the roll period results, changing in heel side and initial heel angle did not have significant influence on damping ratio.

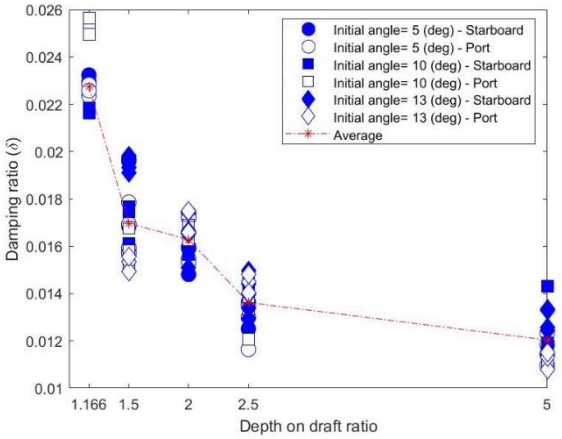

Figure 8. Estimated damping ratio for the container model

Figure 9 presents the percentage increment in roll natural period and damping ratio in comparison with deep water condition (depth to draft ratio of 5) for Hoorn. Despite slightly increase in roll period with the decrease in water depth from d/T of 5 to 2, the change in period was insignificant compared to average period increment at d/T of 1.5 and 1.16ȯ which are 1.3% and 7.6% respectively. The damping ratio has continuously increased with decreasing the water depth. The maximum damping ratio increment has captured at lowest water depth which is 89% larger than the damping ratio in deepest water.

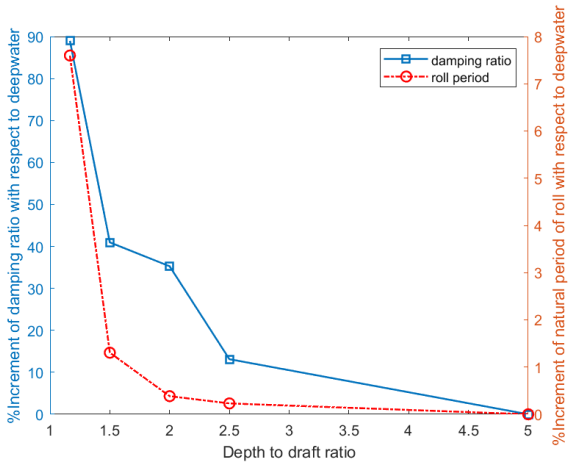

Figure 9. Comparison of percentage increment in average roll natural period and damping ratio of the container model at various depth to draft ratio

Figure 10 to 12 show the estimated linear and nonlinear damping coefficients, by using ITTC recommended procedures. The linear damping coefficient is independent of initial heel angle, however, it increases exponentially with decreasing water depth (Figure 10). According to Figure 11 and 12, nonlinear damping coefficients are around zero, however, the deviation is larger in shallower waters.

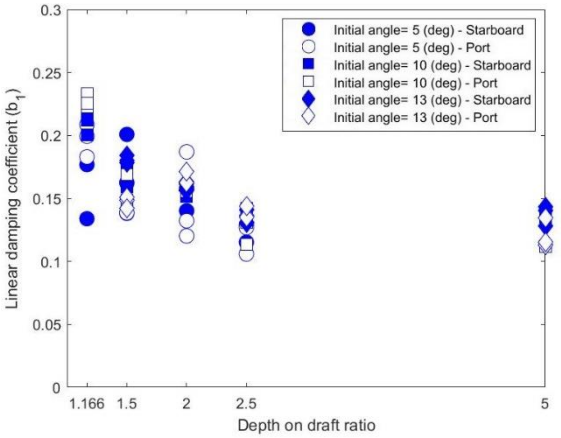

Figure 10. Estimated linear damping coefficient (b_1) for container model by using ITTC recommended procedures

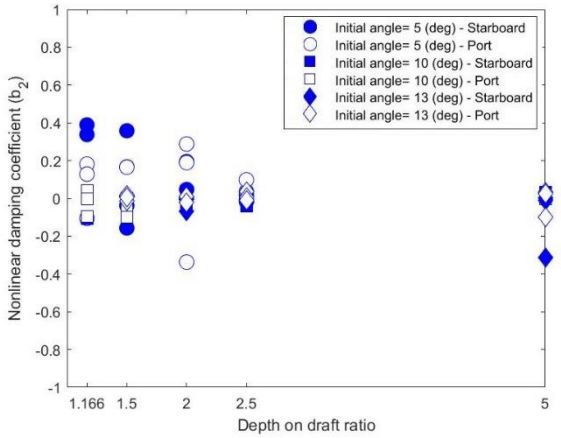

Figure 11. Estimated nonlinear damping coefficient (b_2) for container model by using ITTC recommended procedures

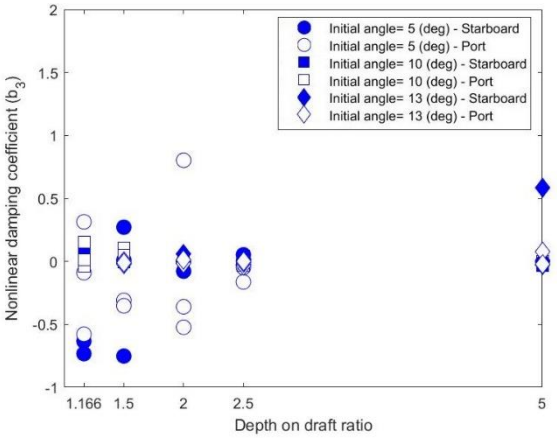

Figure 12. Estimated nonlinear damping coefficient (b_3) for container model by using ITTC recommended procedures

4.3 ROLLING OF MARAD F (BULK CARRIER MODEL)

Having larger C_B, lower centre of gravity and larger roll gyradius, the Marad F (bulk carrier model) was expected to roll relatively faster (smaller roll natural period) compared to the Hoorn. The estimated roll period is shown in Figure 13. Similar to the Hoorn results, changing in heel side and initial angle had no significant effect on the roll period of the Marad F at certain water depth obtained through FFT.

The trend of the water depth effect on roll period and damping for the bulk carrier model is similar to the container model. The estimated damping ratio from roll decay tests for the bulk carrier model is illustrated in Figure 14. Similar to the Hoorn results, with decreasing the water depth the damping ratio of the Marad F exponentially increased and changing in heel side and initial heel angle did not significantly influence the model damping.

Figure shows the percentage increment in roll natural period and damping ratio in deep water condition for Marad F. As show in the Figure , the averaged roll period of Marad F did not alter significantly between d/T of 5 to 2, however, it increased exponentially as the water depth decreased below d/T of 2. It was observed that the deep-water boundary for Marad F occurred at d/T of 2. The roll period of the model in shallowest water was 16.2% more than roll period in deep water. Like the Hoorn model, the damping ratio has continuously increased with decreasing the water depth and the model experienced the maximum damping ratio increment at shallowest water which is about 108% larger than the damping ratio in deepest water.

The estimated linear and nonlinear damping coefficient, by using the recommended procedures by ITTC, at

different water depths are shown in Figure to 18. According to the results, the linear damping coefficient increase exponentially with decreasing the water depth. However, the nonlinear damping coefficients (b_2 and b_3) for the bulk carrier show the same trend as those for the container model. Additionally, the deviation of nonlinear damping coefficients for the bulk carrier are larger than that in the container model.

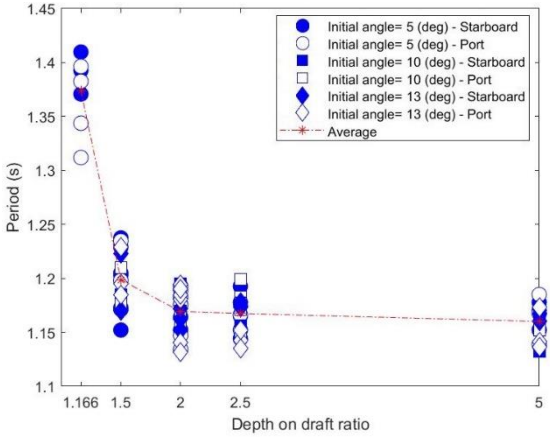

Figure 13. Estimated roll period of the bulk carrier model at different water depth from roll decay tests

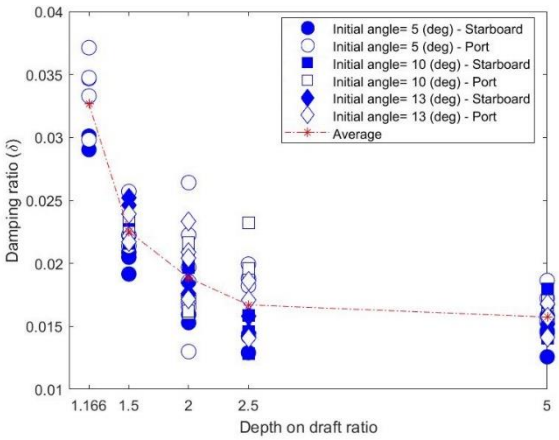

Figure 14. Estimated damping ratio for the bulk carrier model

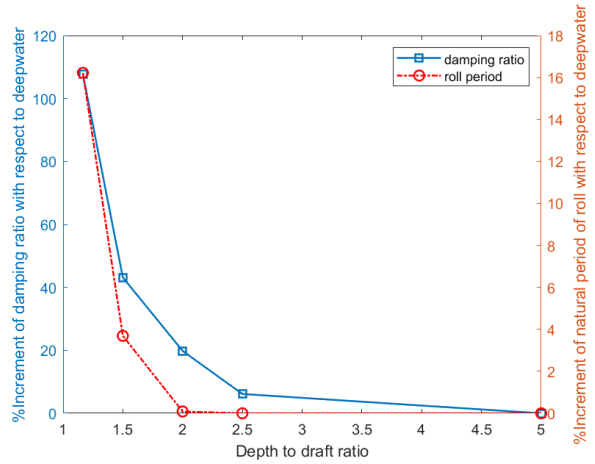

Figure 15. Comparison of percentage increment in average roll natural period and damping ratio of Marad F model at various depth to draft ratio

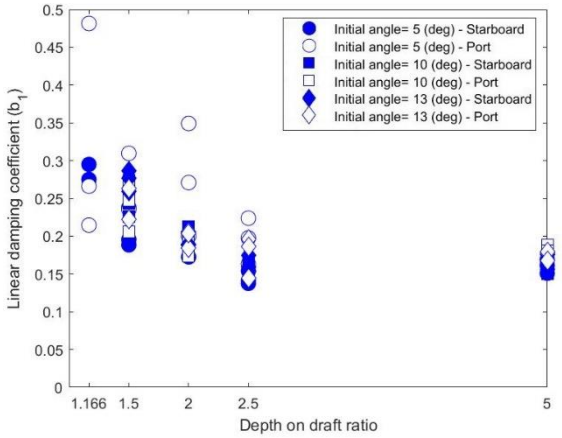

Figure 16. Estimated linear damping coefficient (b_1) for the bulk carrier model by using ITTC recommended procedures

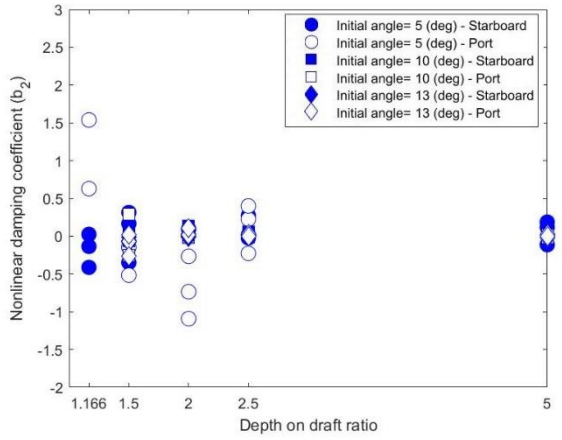

Figure 17. Estimated nonlinear damping coefficient (b_2) for the bulk carrier model by using ITTC recommended procedures

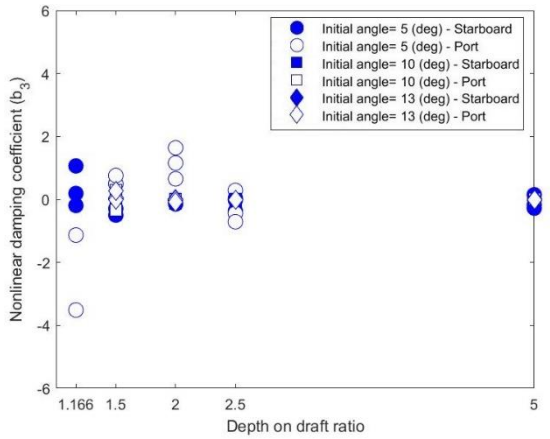

Figure 18. Estimated nonlinear damping coefficient (b_3) for the bulk carrier model by using ITTC recommended procedures

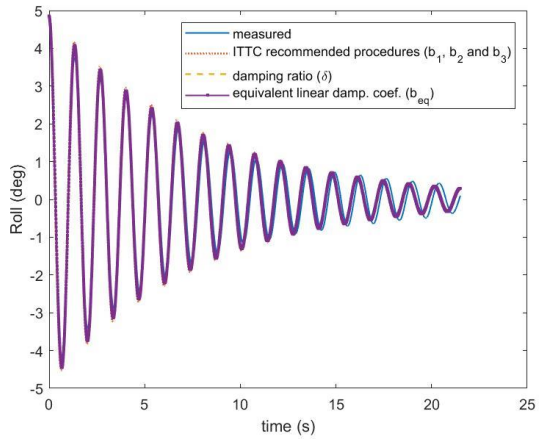

Figure 19. comparing the accuracy of different damping estimation methods for bulk carrier model at depth on draft ratio of 1.16 and initial heel angle of 5 degrees

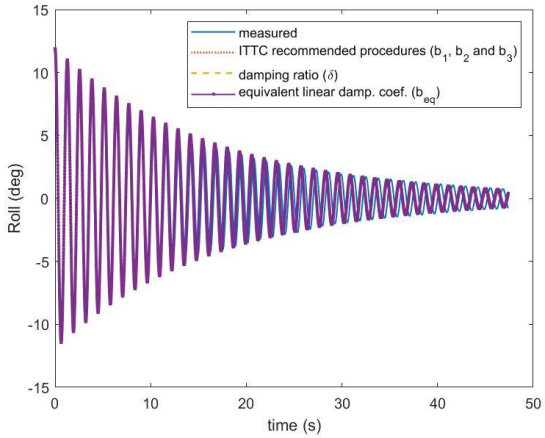

Figure 20. comparing the accuracy of different damping estimation methods for container model at depth on draft ratio of 1.16 and initial heel angle of 5 degrees

4.4 METHODS COMPARISON

As discussed before, different methods were utilised to estimate the roll damping parameters and responses. MATLAB fitting toolbox was applied to fit an exponential curve to the roll decay tests and estimate the damping ratio (δ). ITTC recommended procedures was utilised to estimate the linear and nonlinear damping coefficients as well as equivalent linear roll damping coefficient. To compare the accuracy of these methods, the roll decay curves were regenerated for all estimated damping coefficients and compared with the measurements.

The level of accuracy of all different methods were almost the same for whole range of investigated water depths and initial heel angles for both hull forms. Samples of those comparisons are presented in Figures 19 and 20. Figure 19 presents the roll decays created by different estimated damping coefficients for bulk carrier model at shallowest investigated depth to draft ratio and initial heel angle of 5 degrees. Figure 20 shows similar results for the container model at depth to draft ratio of 5 and initial heel angle of 13 degrees. It should be mentioned that the phase difference between the measurements and the estimations are related to the FFT error.

Since both models were tested with no bilge keel and appendages, they did not show noticeable nonlinear damping terms and it could be the reason of similarity of the results. However, this will be investigated in the future work.

5 CONCLUSION

In order to predict rolling amplitude precisely to prevent risk of grounding of a vessel operating in shallow water, an accurate prediction of roll natural period and damping parameter of the vessel are required. This study focuses on investigating the effect of water depths on the roll natural period of a vessel in calm water condition such as operating on inland waterways. Roll decay tests were undertaken to obtain the roll period of two models (Container ship and Bulk carrier), with different C_B, in calm water condition with zero forward speed. From the experiment, it was shown clearly that the roll period was affected by the change in water depth especially in the shallow water region due to the change in vessel roll added mass moment of inertia.

According to the results, the roll natural period for both models remained approximately unchanged at water depth

to draft ratio of greater than 2.0, however, they increased exponentially with the decrease in water depth for the depth to draft ratio of less than 2.0. The roll natural period of bulk carrier model, with greater C_B, recorded 16.2% increment at d/T of 1.16ȯ, the shallowest tested water depth. In other hand, for Hoorn (container model), the recorded increment was much lower. At d/T of 1.5, the roll natural period of Hoorn has increased not more than 1.5%; and approximately 7.6% at d/T of 1.166.

The damping ratio of the bulk carrier model, with greater C_B, was more prompt to changes by the change in water depth. The decrease in water depth always associated with an increase in damping. The rate of change of damping ratio showed an exponential increase with linear decrement of water depth. The comparison between deepest and shallowest water damping ratio showed a significant increase of 89% and 108% for the container ship and bulk carrier models, respectively.

Investigating the linear and nonlinear damping coefficients individually, showed that for both models the linear damping coefficient exponentially increase with decreasing the water depth, however, the nonlinear terms were around zero for deeper waters and have larger values in shallower waters.

The comparison of the estimated damping coefficients using different methods showed insignificant deviations among the estimated values which mainly related to small value of nonlinear terms. Having no bilge keel and appendages might be the reason for insignificant nonlinear roll damping for both models.

6 ACKNOWLEDGEMENTS

The support of the OMC International and the Australian Maritime College, particularly the in-kind contribution of the Model Test Basin staff, is gratefully acknowledged.

7 REFERENCES

BBC News, 2021, September 1. South America's drought-hit Paraná River at 77-year low. https://www.bbc.com/news/world-latin-america-58408791.

Dawson, E., 2015. An Investigation into the Effects of Roll Gyradius on Experimental Testing and Numerical Simulation: Troubleshooting Emergent Issues. Defence Science and Technology Organisation, DSTO-TN-1402.

Delefortrie, G, Vantorre, M., 2021. 6DOF manoeuvring model of KCS with full roll coupling. Ocean Engineering 235, 109327.

Haddara, M. R., & Wu, X., 1995. Parameter Identification of Nonlinear Rolling Motion in Random Seas. Intl Shipbuilding Progress 46(445), 247–260.

Hansch, D.L., 2015. The Effect of Shallow Water on Roll Damping and Rolling Period. MSc Dissertation, Ocean Engineering, Virginia Polytechnic Institute and State University. pp. 1-44.

ITTC, (2011). Numerical Estimation of Roll Damping. ITTC- Recommended procedures and guidelines, 7.5-02 -07-04.5. Revision 00. 32 pp.

Piehl, H., 2017. Ship roll damping analysis. PhD Thesis, Fakultät für Ingenieurswissenschaften, Abteilung Maschinenbau und Verfahrenstechnik, Universität Duisburg-Essen. pp. 1-178.

Mahfouz, A. B., 2004. Identification of the nonlinear ship rolling motion equation using the measured response at sea. Ocean Engineering 31, 2139-2156.

NASA, 2021, September 27. Drought Makes its Home on the Range. Global Climate Change. https://climate.nasa.gov/news/3117/drought-makes-its-home-on-the-range/

Steffen, W., Hughes, L., Dean A., Martin, R., 2018. Climate Council of Australia Limited. https://www.climatecouncil.org.au/resources/climate-change-and-drought-factsheet/

Taylan, M., 1996. Nonlinear roll motion of ships in beam waves. Bull. Tech. Univ. Istanbul 49, 459-479.

William, W., Lehane, B., Dezem, V., 2019. Rhine River Shipping Faces Another Historic Shutdown as Drought Hits Water Levels. Insurance Journal, July 24. https://www.insurancejournal.com/news/international/2019/07/24/533767.htm.

Zhou, Z.X., Lo, E.Y., Tan, S.K., 2005. Effect of shallow and narrow water on added mass of cylinders with various cross-sectional shapes. Ocean Engineering, 32(10), 1199-1215.

Zwart, W.E., 2017. Analysis of Ship Motions in Shallow Water. Msc Dissertation, Offshore and Dredging Engineering, Delft University of Technology. pp. 1-157.

8 AUTHORS BIOGRAPHY

Dr Javad A. Mehr is a lecturer at the National Centre for Maritime Engineering and Hydrodynamics (NCMEH) of the Australian Maritime College (AMC), an institute of University of Tasmania (Utas). He is also the course coordinator for Marine and Offshore Engineering (MOE) cohort. His previous experience includes ship Ride Control Systems (RCS), hydrofoils, hydrodynamics, seakeeping, model tests, and ship motions and loads.

Dr Mohammadreza Javanmardi holds the current position of Senior Engineer at OMC International. He is responsible for the research and development of algorithms for integrating live ship motion measurement into ship motion predictions. Mohammadreza received his BSc (2005) in Naval Architecture and Maritime Engineering from Amir-Kabir University of Technology, MSc (2008) in Mechanical Engineering from Sharif University of Technology and his Ph.D. (2014) in Hydrodynamics from University of Tasmania, and then served as Lecturer (2015-2016) at AMC and a Postdoctoral associate (2016-2017) at Sharif University of Technology.

Shin Wei Tham graduated with the Bachelor of Engineering (First Class Honours) from the Australian Maritime College, University of Tasmania in December 2021. He specialised in Marine and Offshore Engineering and has special interest in maritime system engineering, ship motion study and reliability engineering. He has experience in operation and maintenance of oil palm biomass boiler (2019) and researched into the effect of water depth on roll motion of merchant ship during his tertiary education (2021).

Yun Yin graduated from University of Tasmania (Australian Maritime College) in December 2021 with an honours bachelor's degree (Marine and Offshore Engineering). He worked for Cara Shipping Pte. Ltd. as a cadet on board bulk carrier MV. Stella Grace (2015-2016). He was under the employment of CSC Jinling Shipyard as an intern (2019-2020).